Respiratory Physiology & Neurobiology 222 (2016) 1–5

Contents lists available at ScienceDirect

Respiratory Physiology & Neurobiology

journal homepage: www.elsevier.com/locate/resphysiol

Expansion of bubbles under a pulsatile flow regime in decompressed ovine blood vessels

Ran Arieli[a,*], Abraham Marmur[b]

[a] Israel Naval Medical Institute, Israel Defence Forces Medical Corps, Haifa, Israel
[b] Department of Chemical Engineering, Technion-Israel Institute of Technology, Haifa, Israel

ARTICLE INFO

Article history:
Received 27 July 2015
Received in revised form 30 October 2015
Accepted 12 November 2015
Available online 22 November 2015

Keywords:
Decompression bubble
Hydrophobic spot
Growth rate
Vascular bubbles

ABSTRACT

After decompression of ovine large blood vessels, bubbles nucleate and expand at active hydrophobic spots on their luminal aspect. These bubbles will be in the path of the blood flow within the vessel, which might replenish the supply of gas-supersaturated plasma in their vicinity and thus, in contrast with our previous estimations, enhance their growth. We used the data from our previous study on the effect of pulsatile flow in ovine blood vessels stretched on microscope slides and photographed after decompression from hyperbaric exposure. We measured the diameter of 46 bubbles in 4 samples taken from 3 blood vessels (pulmonary artery, pulmonary vein, and aorta) in which both a "multi-bubble active spot" (MBAS)—which produces several bubbles at a time, and at least one "single-bubble active spot" (SBAS)—which produces a single bubble at a time, were seen together. The linear expansion rate for diameter in SBAS ranged from 0.077 to 0.498 mm/min and in MBAS from 0.001 to 0.332 mm/min. There was a trend toward a reduced expansion rate for bubbles in MBAS compared with SBAS. The expansion rate for bubbles in an MBAS when it was surrounded by others was very low. Bubble growth is related to gas tension, and under a flow regime, bubbles expand from a diameter of 0.1 to 1 mm in 2–24 min at a gas supersaturation of 620 kPa and lower. There are two phases of bubble development. The slow and disperse initiation of active spots (from nanobubbles to gas micronuclei) continues for more than 1 h, whereas the fast increase in size (2–24 min) is governed by diffusion. Bubble-based decompression models should not artificially reduce diffusion constants, but rather take both phases of bubble development into consideration.

1. Introduction

We have shown that after decompression of ovine large blood vessels from high pressure, bubbles nucleate and expand at active hydrophobic spots on their luminal aspect (Arieli and Marmur, 2013, 2014; Arieli et al., 2015). We suggested that these active spots are the principal source of bubbles which cause the most severe decompression sickness. Various features of diving can be explained by this mode of bubble formation: bubblers–nonbubblers, adaptation to diving, a greater risk of decompression sickness on the second dive, and CNS decompression sickness (Arieli et. al., 2015). The rate of bubble expansion after decompression has been studied in the past, both theoretically and experimentally, in calm conditions (Arieli and Marmur, 2014; Kim et al., 2004; Kwak and Kim, 1998; Nikolaev, 2000; Papadopoulou et al., 2015). In some of these investigations, blood perfused the tissue encompassing the bubble. However, none of them studied the flow of the medium surrounding the bubble. Bubbles on the luminal aspect of blood vessels will be in the path of blood flow, which might replenish the supply of gas-supersaturated plasma in their vicinity. In such a case, gas transfer into the bubble will no longer be limited by diffusion through the surrounding medium, and the growth rate of a bubble adhering to the blood vessel wall should in reality be faster than previously estimated. Some studies refer to the competition for gas between adjacent bubbles (Chappell and Payne, 2006; Papadopoulou et al., 2015; Van Liew and Burkard, 1993). However, the flow of the medium may obliterate the diffusion distance prevailing in calm conditions, and therefore reduce or eliminate the competition for dissolved gas between adjacent bubbles. In our last report (Arieli et al., 2015), we photographed decompressed blood vessels in calm conditions for the first 30 min, and then in pulsatile flow of supersaturated saline with a mean velocity of 234 cm/min. Bubble expansion after decompression was

* Corresponding author at: Klil Hakhoresh 12, Rakefet, D. N. Misgav 2017500, Israel. Fax: +972 4 9801210.
E-mail address: rarieli@netvision.net.il (R. Arieli).

http://dx.doi.org/10.1016/j.resp.2015.11.010
1569-9048/

extracted from the records of this study for the measurement of growth rate. Because there are active spots which produce a single bubble at a time, the single-bubble active spot (SBAS), and others which produce a number of bubbles at the same time, the multi-bubble active spot (MBAS), the growth of a single bubble can be compared with the growth of a number of bubbles adjacent to one another on the same active spot. In the present report, we describe the growth rate of bubbles under pulsatile flow of saline. We also suggest two steps of bubble expansion, a slow phase followed by a fast phase.

2. Methods

The methods were described in detail in our previous report (Arieli et al., 2015), and will be presented briefly here.

2.1. Tissue preparation

The complete heart and lungs from 6 slaughtered sheep (taken on separate days) were obtained at the abattoir. In the laboratory, under saline and without any exposure to air, samples from the blood vessels were gently stretched on microscope slides using metal clips with the luminal aspect exposed. Two slides were placed on the bottom of two Pyrex bowls (diameter 26 cm, height 5 cm) under 2.5 cm saline. The other two slides were kept under saline in the refrigerator for the next day.

2.2. 2 Protocol

The bowls containing the samples were transferred to two different 150 L hyperbaric chambers and were placed on double-walled metal plates with circulating water at 12° C for tissue preservation. Beforehand, the air conditioning in the small room containing the two hyperbaric chambers was used to take the room temperature down to 15° C. Staining for lipids following the 20 h exposure proved that the phospholipids layers at the active spot on the luminal aspect of the blood vessels remained intact (Arieli el al., 2015). Pressure was elevated at a rate of 200 kPa/min to 1013 kPa, 90 m sea water, and remained at that pressure overnight (20.5 ± 2.3 h, mean $\pm$ SD). In the morning, one of the chambers was decompressed at a rate of 200 kPa/min. The bowl was placed carefully on a nearby table for photography. We started automated photographing at 1-s intervals. The first 30 min of photography was conducted in calm conditions. Photography was resumed for the second 30 min with a flow of saline delivered horizontally over the blood vessel at a rate of 234 cm/min using a peristaltic pump. The same protocol was followed for the other samples.

Three blood vessels were examined, the aorta, pulmonary artery, and pulmonary vein, in which both an MBAS and at least one SBAS were seen together. The diameter of bubbles was measured under pulsatile flow at selected time intervals (0.25–1 min, according to their growth rate) over a period of 8–16 min. Because it usually takes time in the flow protocol until an MBAS is seen clearly, in three of the four samples the sampling period started some time after the pump had been switched on. Four samples were taken from 3 blood vessels, comprising 46 bubbles. Arieli and Marmur (2014) used a simple model to calculate bubble expansion after decompression. This model predicted linear growth of the diameter of a spherical bubble with time. The model assumed a constant diffusion distance and gas tension. The effect of surface tension was not considered. Although this is not the case in calm conditions, the actual diameters changed in a linear mode with time even in the calm state (Arieli and Marmur, 2014). When the medium flows over the bubbles, as in the present case, and it is well mixed, the diffusion path should be small. One would therefore expect linearity of the diameter with time, and the slope for diameter as a function of time was calculated for each bubble. Gas tension may decrease with time, mainly due to bubbles formed by the pump and depletion of the dissolved gas. Thus, the driving pressure for gas loading in the bubble should decrease with time.

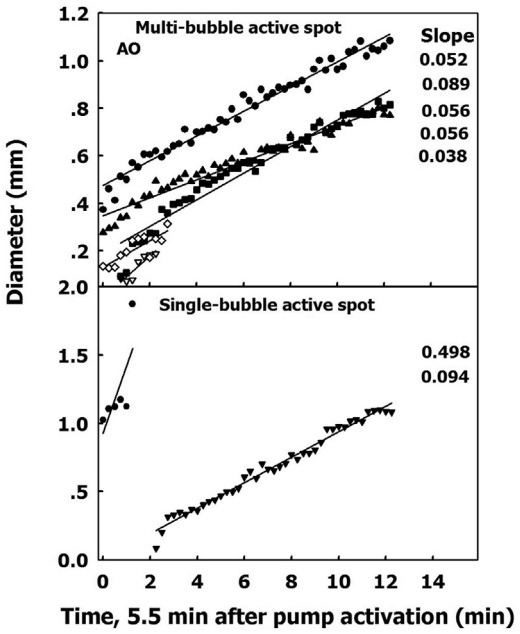

Fig. 1. Diameter of bubbles in the aorta (AO) for one single-bubble active spot (SBAS, lower panel) and one multi-bubble active spot (MBAS, upper panel) as a function of time. Each symbol represents a bubble. After the first bubble detached from the SBAS, another bubble developed. Slopes of the linear regression for each bubble are shown.

2.3. Statistical analysis

Univariate ANOVA and Levene's test for equality of variances were used to compare expansion rates on the SBAS and MBAS for the four samples.

3. Results

The size of bubbles in the sampled aorta is shown in Fig. 1, with the diameter of bubbles on the SBAS appearing in the lower panel. After detachment of the first bubble, another started developing on the same spot. Initially (over the first 3 measurements) the expansion rate of the second bubble (full triangles) was high, becoming lower as time progressed. The slope of the first bubble was steeper than that of the second, ranging from 0.094 to 0.498 mm/min (mean 0.296). A similar rate of expansion was observed over the same period (starting from the time the pump was activated) for 5 bubbles on the MBAS (upper panel), ranging from 0.038 to 0.089 mm/min (mean 0.058). Two bubbles which persisted for only a short time (empty symbols) did not detach, but merged with the larger bubble close by, resulting in a sudden steep increase in its diameter (full square symbols). In two bubbles (full square and full circle) a steep increase in diameter was seen at the start, with a more gradual slope as time progressed. The distance between the SBAS and MBAS was 5.0 mm.

Results from two SBAS and one MBAS in the pulmonary artery are shown in Fig. 2. Linear growth rates (slopes) were variable for the bubbles on both of the SBAS and for five bubbles on the MBAS, ranging from 0.057 to 0.123 mm/min (mean 0.090) on the SBAS and from 0.10 to 0.096 mm/min (mean 0.058) on the MBAS. The delay to sampling (time from pump activation) in this case was twice as

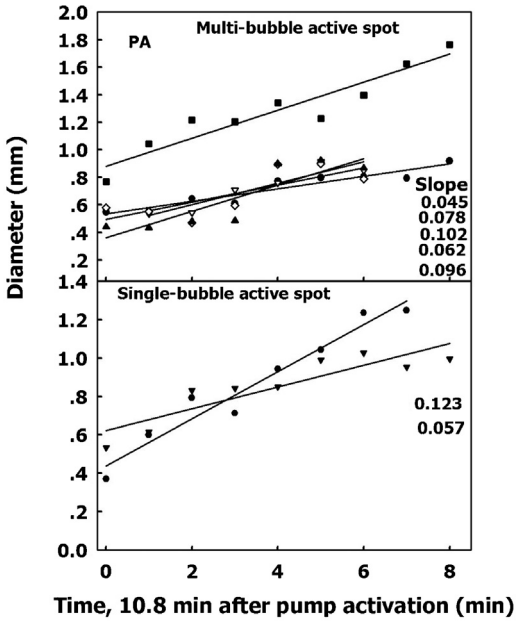

Fig. 2. Diameter of bubbles in the pulmonary artery (PA) for two SBAS (lower panel) and one MBAS (upper panel) as a function of time. Other symbols are as in Fig. 1.

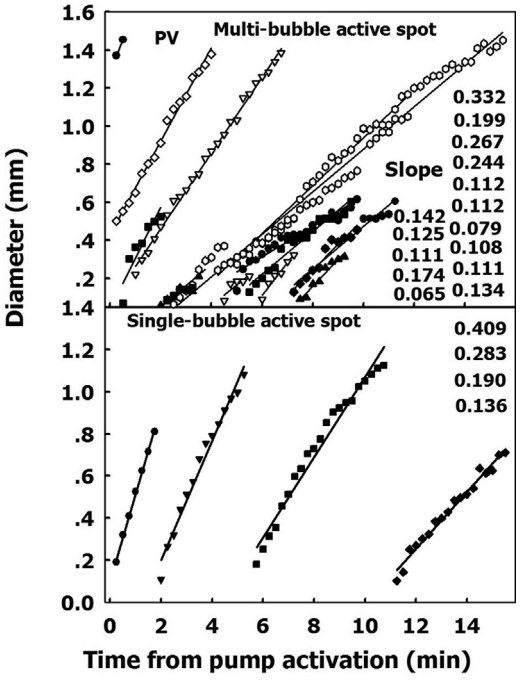

Fig. 3. Diameter of bubbles in the pulmonary vein (PV) for one SBAS (lower panel) and one MBAS (upper panel) as a function of time from the start of pump activation. After the detachment of large bubbles, other bubbles developed in their place. Other symbols are as in Fig. 1.

long as in Fig. 1, and no change was observed in the gradient of each slope. The two SBAS were situated 6.0 and 8.4 mm from the MBAS.

Results from one SBAS and one MBAS from the pulmonary vein, when the sampling period started from the time the pump was activated, are shown in Fig. 3. In the SBAS four bubbles were created on the same spot, one after the other. The linear expansion rate decreased with the sequence of bubbles. During the same period of time, 15 different bubbles appeared on the MBAS. The steep slope 0.332 refers to the two measurements taken at the start. When one bubble (full black circle) merged with another (open circle,

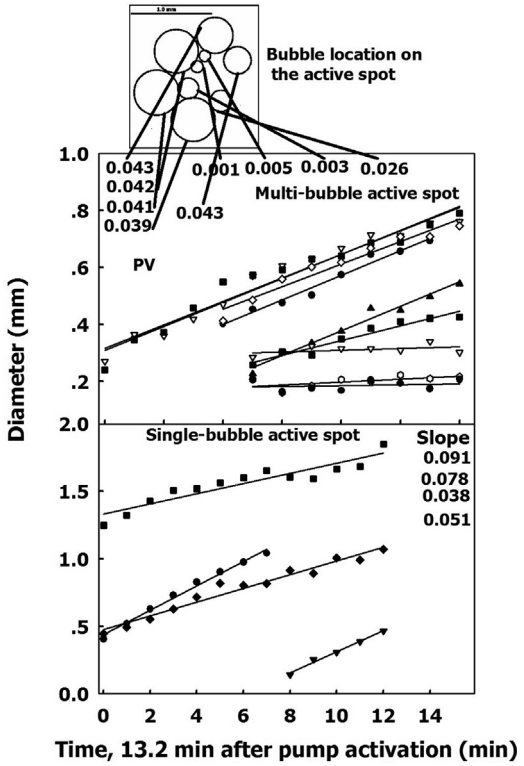

Fig. 4. Diameter of bubbles in the pulmonary vein (PV) for three SBAS (lower panel) and one MBAS (upper panel) as a function of time, 13.2 min from pump activation. After the detachment of large bubbles, other bubbles developed in their place. Other symbols are as in Fig. 1. The constellation of bubbles on the MBAS is shown above the upper panel to a scale of 1 mm, and with lines connecting each bubble to its slope.

lower sequence), a sudden steep increase was seen in the diameter of the latter. The slopes of the bubbles which appeared earlier were steeper than those which appeared later. For the SBAS, the slope ranged from 0.136 to 0.409 mm/min (mean 0.255), and for the MBAS from 0.065 to 0.332 mm/min (mean 0.154). The distance between the SBAS and MBAS was 4.8 mm.

Results from three SBAS and one MBAS from the pulmonary vein, when the sampling period started 13.2 min after pump activation, are shown in Fig. 4. In the SBAS, the slope of a bubble which detached after about 6.5 min (full circles), 0.091, was steeper than that of the following bubble (full triangles) from the same SBAS, 0.051. Variable slopes were seen for the 9 bubbles which formed on the MBAS. The actual arrangement of bubbles on the spot is depicted above this panel to a scale of 1 mm. Lines connect each bubble to its slope. It can be seen that the linear expansion rate was almost zero for bubbles which were surrounded by others. The slopes for the SBAS ranged from 0.051 to 0.091 mm/min (mean 0.065), and for the MBAS from 0.001 to 0.043 mm/min (mean 0.025). The three SBAS were situated 4.8, 6.9 and 11.4 mm from the MBAS.

The power of the statistical analysis was low because of the small amount of data. Univariate ANOVA yielded a non-significant difference between expansion rates for the SBAS and MBAS. A trend was seen toward a reduced rate for the MBAS compared with the SBAS. When the *t*-test was used for each sample (assuming either equal or non-equal variance), a significant difference was found between expansion rates for the SBAS and MBAS in the pulmonary vein when measurement started 13.2 min after the pump was activated ($P > 0.011$ and $P < 0.043$, respectively).

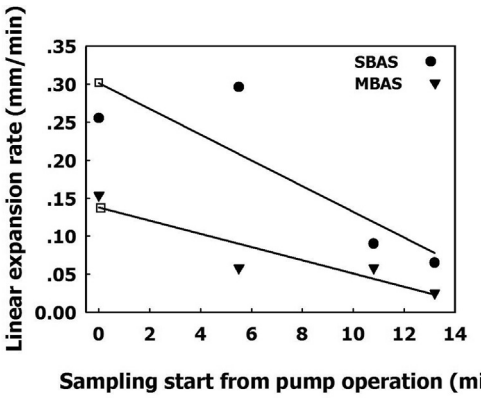

Fig. 5. Mean linear expansion (slope) as a function of the time from pump activation for both single-bubble active spots—SBAS circles, and multi-bubble active spots—MBAS triangles.

4. Discussion

4.1. Gas depletion reduces growth rate

Gas should be depleted fast when the pump is operating due to the bubbles it produces. In our simple model, we assumed a constant gas tension (Arieli and Marmur, 2014). Therefore the slope should decline with time during operation of the pump. This can be clearly seen in the SBAS in the lower panels of Figs. 1, 3 and 4. An initial steep slope which declined as time progressed may be noted for the full squares in the upper panel and full triangles in the lower panel of Fig. 1, and for the sequence of slopes in the upper panel of Fig. 3. The mean slope was also more gradual when the sampling period started later (Fig. 5). We conclude quite simply that the rate of bubble expansion was related to gas tension: a reduction of tension with time also reduced the expansion rate.

4.2. Competition for gas

Other studies have examined the competition for gas between adjacent bubbles (Chappell and Payne, 2006; Papadopoulou et al., 2015; Van Liew and Burkard, 1993). We assumed that during flow, a medium rich in gas would reach all the bubbles. However, it can be seen that bubbles which were surrounded by others did not expand (Fig. 4), and that the linear expansion rate was lower for the MBAS than it was for the SBAS (Fig. 5). Thus even under a flow regime, adjacent bubbles compete for the dissolved gas. Small bubbles which are under the shadow of larger ones do not receive their share of the dissolved gas, which is snatched up by the larger bubble (Fig. 4). A similar finding of reduced growth rate in adjacent bubbles in calm conditions was reported by Papadopoulou et al. (2015).

4.3. Expansion rate is related to gas tension

If only a small amount of gas were depleted from the saline during the 30 min of calm conditions, the gas tension in the well-mixed saline at the start of pump operation should still amount to 620 kPa (Appendix A, Arieli et al., 2015). Extrapolating the mean slopes to the start of pump operation (empty square, Fig. 5) yields a linear expansion rate of 0.30 mm/min for the SBAS and 0.14 mm/min for the MBAS. Thus, at a gas tension of 620 kPa it would take a 0.1 mm diameter bubble 3 min to reach the detachment diameter of 1.0 mm on an SBAS and 6.4 min on an MBAS. These time spans are much shorter than the 11 min in calm conditions (Arieli and Marmur, 2014), when gas tension in the vicinity of the bubble was only 220 kPa. Ninety percent of the rates of expansion for the increase in diameter from 0.1 to 1 mm (excluding 10% of bubbles which were surrounded by others), would extend over a time span of 2–24 min as gas tension is reduced. Transforming the squared time data for growth rate from Papadopoulou et al. (2015) into a linear relation yields slopes of 0.059–0.094 mm/min for a gas tension of 304 kPa (10–15 min for expansion from 0.1 to 1 mm). These values are within the range reported here.

4.4. Volume increases with time

The rate of expansion for the 46 bubbles in this report agrees with linearity. If we take into account the short time (2–24 min) in which bubbles grew and became detached, and the long time required for the removal of loaded nitrogen after diving, we would be correct to assume linear expansion of bubble radius with time at the blood vessel wall. Evidently, the volume of the detached bubble, as well as the number of bubbles and their location, is the main cause of decompression sickness (Flook, 2000; Hugon, 2014). Thus the increase in volume over time as the bubble increases in diameter from 0.1 mm should be $(4/3)\pi[0.05+(a/2)t]^3$, where a is the linear expansion rate of the diameter.

4.5. Expansion of arterial bubbles

In the present study, there was no difference in bubble growth rate between the pulmonary vein and the aorta, vessels which in vivo contain arterial blood, and the pulmonary artery and the vena cava, which contain venous blood, nor were there differences in the abundance of active spots (Arieli et al., 2015). However, the actual growth rate of bubbles should be lower within the arterial than within the venous circulation, due to the release of nitrogen by the venous blood as it passes the lung capillaries. Nevertheless, expansion of arterial bubbles may occur because the tissue surrounding the arterial vessels is rich in nitrogen, which will diffuse through the arterial walls to the arterial blood, enriching it with nitrogen along the arterial pathway. Thus the expansion rate of arterial bubbles will increase with the distance from the lung along the arterial tree. Expansion of arterial bubbles at some distance from the left ventricle, may explain why microembolic signals count in cerebral arteries did not correlate with the arterial bubble grades in the left heart (Barak et al., 2015).

4.6. Two-phase bubble evolution

Fast expansion of a bubble from a diameter of 0.1 mm to its size of 1 mm on detachment, which takes from 2 to 24 min (Figs. 2–4), is obviously preceded by a much slower process for transformation of the nanobubble into a gas micronucleus. This finding may explain the discrepancy which arose in the calculation of decompression models, when researchers matched bubble growth with decompression bubbles or symptoms. In these decompression models, there was a need to artificially assume a very low diffusion constant in order to enable such a match (Hugon, 2014; Nikolaev, 2013).

We suggest replacing what would appear to be a questionable assumption with our two-stage process:

1. A slow process, in which nanobubbles are transformed into gas micronuclei. We term this stage “the initiation of active spots”, which goes on for more than 1 h after decompression (Arieli et al., 2015). Papadopoulou et al. (2015) reported that all the sites which produced bubbles, either in muscle or in fat tissue, were seen within 10 min of decompression. The discrepancy between that study and the present investigation may be related to the source of the gas micronuclei. The tissues in the preparation examined by Papadopoulou et al. (2015) were exposed to air. This may have led to some cavities on the tissue surface taking

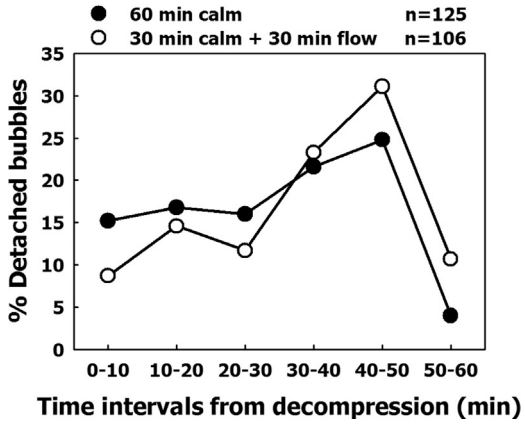

Fig. 6. The percentage of first bubble detachments from the active spots as a function of time from decompression for 1 h in calm condition (13 sheep), and 0.5 h in calm conditions followed by 0.5 h in flow conditions (6 sheep). The number of active spots is represented by *n*.

up gas, which later served as gas micronuclei. In our preparation, there was no exposure to air at all, and gas micronuclei developed on the active hydrophobic spots.

2. Fast expansion of the gas micronucleus until it becomes a fully developed bubble, without any deviation of the diffusion constant.

One can get a glimpse of the evolution of the slow phase in Fig. 6, where the distribution of first detachments from the active spots is presented as a function of time from decompression (data extracted from Arieli et al., 2015). Thus, initiation of the active spot could have started about 10 min before detachment. In both conditions, the first detachment peaked at the 40–50 min time interval and declined thereafter. Subtracting the time taken by the fast phase would yield the slow phase. In real decompression from a dive, the release of dissolved gas should be slower than in our experimental setup and the initiation phase might therefore be extended. Hugon (2014) reviewed different decompression models and suggested that "vascular bubble models, proposing a realistic biophysical approach, are promising for the prevention of decompression sickness and the devising of suitable decompression procedures." He also claimed: "Physical artifacts such as very low diffusion coefficients were sometimes introduced to slow down the bubble growth process, in order to echo the observed DCS symptom delay. This assumption remains questionable." Therefore, using our time relationship for the initiation of active spots (Fig. 6), with their subsequent activation (Fig. 7, Arieli and Marmur, 2014) and bubble growth that is in line with the correct physical coefficients, might yield Hugon's expected model. Further sophistication might include the reduction of active spots in experienced divers (Arieli et al., 2015).

5. Conclusions

1. Under a flow regime, bubbles expand from a diameter of 0.1 to 1 mm in 2–24 min at a gas supersaturation of 620 kPa and lower.
2. Expansion rate will decrease with the reduction in gas supersaturation.
3. The rate of expansion in adjacent bubbles which are exposed largely to the flow medium is close to that of single bubbles.
4. Growth rate is reduced in bubbles surrounded by others.
5. There are two phases of bubble development: the slow and disperse initiation of active spots (transformation of nanobubbles into gas micronuclei) and their activation, and a fast increase which is governed by diffusion.

Acknowledgements

The authors thank Mr. R. Lincoln for skillful editing of the manuscript. This study was supported in part by a grant from the IDF Medical Corps and the Israel MOD.

References

Arieli, R., Marmur, A., 2013. Evolution of bubbles from gas micronuclei formed on the luminal aspect of ovine large blood vessels. Respir. Physiol. Neurobiol. 188, 49–55.
Arieli, R., Marmur, A., 2014. Ex vivo bubble production from ovine large blood vessels: size on detachment and evidence of active spots. Respir. Physiol. Neurobiol. 200, 110–117.
Arieli, R., Arieli, U., Marmur, A., 2015. Bubble size on detachment from the luminal aspect of ovine large blood vessels after decompression: the effect of mechanical disturbance. Respir. Physiol. Neurobiol. 216, 1–8.
Barak, O.F., Madden, D., Lovering, A.T., Lambrechts, K., Ljubkovic, M., Dujc, Z., 2015. Very few exercise-induced arterialized gas bubbles reach the cerebral vasculature. Med. Sci. Sports Excer. 47, 1798–1805.
Chappell, M.A., Payne, S.J., 2006. A physiological model of the interaction between tissue bubbles and the formation of blood-borne bubbles under decompression. Phys. Med. Biol. 51, 2321–2338.
Flook, V., 2000. The physics and physiology of decompression. Eur. J. Underwater Hyperbaric Med. 1, 1–8.
Hugon, J., 2014. Decompression models: review, relevance and validation capabilities. Undersea Hyperb. Med. 41, 531–556.
Kim, K.Y., Kang, S.L., Kwak, H.-Y., 2004. Bubble nucleation and growth in polymer solutions. Polym. Eng. Sci. 44, 1890–1899.
Kwak, H.-Y., Kim, Y.W., 1998. Homogeneous nucleation and macroscopic growth of gas bubble in organic solutions. Int. J. Heat Mass Transf. 41, 757–767.
Nikolaev, V.P., 2000. Effects of heterogeneous structure and diffusion permeability of body tissues on decompression gas bubble dynamics. Aviat. Space Environ. Med. 71, 723–729.
Nikolaev, V.P., 2013. Simulation of gas bubble growth and dissolution in human tissues during dives and recompression. Aviat. Space Environ. Med. 84, 938–945.
Papadopoulou, V., Evgenidis, S., Eckersley, R.J., Mesimeris, T., Balestra, C., Kostoglou, M., Tang, M.-X., Karapantsios, T.D., 2015. Decompression induced bubble dynamics on ex vivo fat and muscle tissue surfaces with a new experimental set up. Colloids Surf. B Biointerfaces 129, 121–129.
Van Liew, H.D., Burkard, M.E., 1993. Density of decompression bubbles and competition for gas among bubbles, tissue, and blood. J. Appl. Physiol. (1985) 75, 2293–2301.